Desalination and Water Treatment
www.deswater.com

doi: 10.5004/dwt.2019.24563

163 (2019) 96–108
September

Degradation of chloramphenicol by Ti-Ag/γ-Al_2O_3 particle electrode using three-dimensional reactor

Yongjun Sun[a,*], Aowen Chen[a], Wenquan Sun[a], Jun Zhou[a], Kinjal J. Shah[a], Huaili Zheng[b], Hao Shen[a]

[a]*College of Urban Construction, Nanjing Tech University, Nanjing, 211800, China, emails: sunyongjun@njtech.edu.cn (Y. Sun), 1064442347@qq.com (A. Chen), coneflower@163.com (W. Sun), zhoujun0913@126.com (J. Zhou), kinjalshah8@gmail.com (K.J. Shah), 2508688193@qq.com (H. Shen)*

[b]*Key laboratory of the Three Gorges Reservoir Region's Eco-Environment, State Ministry of Education, Chongqing University, Chongqing, 400045, China, email: zhl@cqu.edu.cn*

Received 225 January 2019; Accepted 13 June 2019

ABSTRACT

In this paper, highly efficient Ti-Ag/γ-Al_2O_3 particle electrodes were prepared for efficient degradation of chloramphenicol (CAP) by using three-dimensional electrocatalytic technology. The effects of preparation factors, such as mass ratio of Ti/Ag, loading times, and calcination temperature, on the electrocatalytic performance of Ti-Ag/γ-Al_2O_3 particle electrode were investigated. In addition, Ti-Ag/γ-Al_2O_3 particle electrodes under different conditions were characterized by SEM, EDS, XRF, and XRD. The optimal removal rate of chloramphenicol was 84.2% with initial concentration of chloramphenicol 100 mg/L, conductivity 6,000 μs cm^{-1}, initial pH 4.0, current intensity I = 0.2 A, and flow rate 1.0 L/min. The elimination of •OH by addition of *t*-butanol reduced the chloramphenicol removal rate by 56.0% under the same working conditions, indicating that the degradation of chloramphenicol was caused by the combination of •OH indirect oxidation and anodic indirect oxidation. Meanwhile, the degradation process of chloramphenicol was approximately in accordance with the first-order kinetic equation.

Keywords: Electrocatalysis; Particle electrode; Degradation; Chloramphenicol

1. Introduction

In recent years, with the rapid development of society, chlorine-containing organic substances are widely used in human production and life, and their adverse effects on the environment are increasing [1]. At the same time, the chlorine-containing organic matter has the characteristics of strong fat solubility and certain biological toxicity, and it is difficult to degrade by biochemical methods, which may cause immeasurable damage to human health [2]. Therefore, the problem of ecological environment pollution control of chlorine-containing organic substances has gradually attracted worldwide attention of experts [3]. Chloramphenicol is a broad-spectrum antibiotic produced with strong toxic effects and side effects. Residual chloramphenicol will eventually be enriched in the human body through the food chain [4]. Long-term chloramphenicol adverse effects will damage the body's healthy flora system, resulting in disease and harm to health [5].

At present, the treatment technologies for chloramphenicol wastewater mainly include biochemical treatment technology, and physical and chemical treatment technology [6]. Biochemical treatment technology mainly uses the biological enzymes produced by microorganisms during growth

* Corresponding author.

or reproduction to catalyze the degradation of organic matter in water, and finally turns the organic matter into the energy and self-nutrients required for survival, thereby achieving the purpose of removing pollutants [7]. However, chloramphenicol has the characteristics of inhibiting microbial growth and biodegradation, and thus improving the activity of related enzymes, and rationally controlling the concentration of chloramphenicol wastewater has become a serious problem [8]. In addition, activated carbon is the most widely used adsorbent, but the price of activated carbon is high, and its regeneration is difficult, which limits its large-scale application [9]. Fenton method uses H_2O_2 and Fe^{2+} in acidic water to form hydroxyl radicals, which in turn have strong oxidative •OH oxidation for degrading organic matter in wastewater [10]. Regardless of the traditional Fenton or electro-Fenton technology, the disadvantages of high power consumption and large amount of excess sludge are not conducive to reduce the operating cost [11]. Therefore, it is very important to seek an efficient and low-cost chloramphenicol treatment process.

Compared with traditional biochemical, adsorption, oxidation and other technical means, the three-dimensional electrocatalyst technology has the advantages of no need to add chemicals, convenient operation, small floor space, mild reaction conditions, diversified functions, high degradation efficiency and no secondary pollution [12]. Therefore, three-dimensional photoelectrocatalysis technology is also known as "environmentally friendly" technology. In recent years, three-dimensional photoelectrocatalytic technology has shown good development prospects in the field of organic refractory wastewater treatment, but there have been few reports on the use of three-dimensional photocatalytic degradation of chloramphenicol wastewater [13].

The three-dimensional electrode is developed on the basis of the traditional two-dimensional electrode, which is filled with a particle material between the conventional two-dimensional electrode cell plate as a three-dimensional particle electrode [14]. Due to the addition of a large number of particle electrodes, after the reactor is energized, its surface is charged due to electrostatic induction or charge conduction, so that each small particle electrode is equivalent to a micro battery, thereby increasing the specific surface area of the reaction [13]. The distance between the contaminant and the plate is shortened, the mass transfer distance is shortened, and the current efficiency is effectively improved [15]. On the other hand, during the electrolysis process, a large amount of highly reactive active radicals are generated on the surface of the particle electrode, thereby no selectively oxidizing most of the organic matter and improving the degradation efficiency of organic matter [16]. More than 70.0% of chloramphenicol was degraded under the optimal conditions using Ti-Sn/γ-Al_2O_3 particle electrodes with a three-dimensional reactor [17]. The high electrocatalytic activity of the UV treated TiO_2 nanotubes was further confirmed by the electrochemical oxidation of persistent organic pollutants, and the total organic carbon analysis revealed that over 90.0% 4-aminophenol was removed when the UV-treated TiO_2 nanotube electrode was employed [18]. Under the optimal conditions, 42.0% and 80.0% of Bisphenol A were removed in the presence of bicarbonate and carbonate using DSA-Ti electrode, respectively [19]. An almost total mineralization with 95.5% total organic carbon removal was achieved for a 1.03 mM 4-hydroxyphenylacetic acid solution at 100 mA cm^{-2} using boron-doped diamond anodes [20].

In this paper, a high-efficiency Ti-Ag/γ-Al_2O_3 particle electrode is prepared and used to remove chloramphenicol by using three-dimensional electrocatalytic oxidation reactor, which provides a new idea for the degradation of chloramphenicol. The effects of preparation factors, such as mass ratio of Ti/Ag, loading times, and calcination temperature, on the electrocatalytic performance of Ti-Ag/γ-Al_2O_3 particle electrode are investigated. In addition, Ti-Ag/γ-Al_2O_3 particle electrodes under different conditions are evaluated by SEM, EDS, XRF, XRD, and BET. The effect of operation condition, such as solution conductivity, initial pH, current intensity, air flow rate, and chloramphenicol concentration, on the degradation of chloramphenicol is explored.

Verification tests of direct and indirect oxidation have been studied in detail, and the kinetics of electrocatalytic oxidation has been investigated.

2. Materials and methods

2.1. Materials

Sulfuric acid (Tianjin Damao Chemical Reagent Factory), sodium hydroxide (Chengdu Kelong Chemical Reagent Factory), nitric acid (Nanjing Chemical Reagent Co. Ltd.), butyl titanate (National Pharmaceutical Group Chemical Reagent Co. Ltd.), silver nitrate ((Chinese medicine) Group Chemical Reagent Co. Ltd.), anhydrous sodium sulfate, chloramphenicol, glacial acetic acid, γ-Al_2O_3, ethanol (Nanjing Chemical Reagent Co. Ltd.), and tert-butanol (Sinopharm Chemical Reagent Co. Ltd.) are of analytical grade and used as received. The deionized water is used throughout the experimental tests.

2.2. Preparation and characterization of Ti-Ag/γ-Al_2O_3 particle electrode

The characteristic parameters of γ-Al_2O_3 are shown in Table S1. γ-Al_2O_3 particles are placed in acetone solution for 15 min to remove organic matter on the surface, and then boiled for 30 min in a certain concentration of dilute nitric acid to remove the oxide layer on the surface. The γ-Al_2O_3 particles after pretreatment are rinsed by distilled water to wash away other impurities. The cleaned γ-Al_2O_3 particles are drained and dried in an oven at 105°C for 12 h. Butyl titanate is added to an anhydrous ethanol-$AgNO_3$ solution with acetic acid as a stabilizer, slowly adding a small amount of distilled water to form a Ti-Ag sol solution under rapid stirring. And the pretreated γ-Al_2O_3 particles are immersed into the prepared Ti sol solution with mixing for 4 h at a constant speed of 120 r/min and 25°C in the water baths shaker. The impregnated γ-Al_2O_3 particles are dried in an oven at 60°C for 12 h until the surface is dry. The dried γ-Al_2O_3 particles are placed in a muffle furnace and calcined at a constant temperature for 4 h. After repeating the above impregnation, drying, and activation steps several times, the Ti-Ag/γ-Al_2O_3 particle electrodes used in the experiment are obtained.

SEM and EDX (FEI Quanta 200, FEI Company, Netherlands) are mainly used to analyze the microstructure and elemental composition of the surface of the particle electrode

to determine whether the active element is successfully loaded on the particle. XRF (Advant XP, ARL Company, Swiss) is used to analyze the composition of the elements in Ti-Ag/γ-Al_2O_3 particle electrodes layer. According to the analysis results, the load elements can be quantitatively and qualitatively analyzed. XRD (Smartlab TM 9KW, Japan Science Corporation, Japan) is a commonly used material structure analysis method, and mainly used to analyze the crystal structure of Ti-Ag/γ-Al_2O_3 particle electrodes.

2.3. Electrocatalytic oxidation tests

In this experiment, chloramphenicol simulated wastewater is used as experimental water. The pH of the wastewater is adjusted by formulating 1.0 mol/L H_2SO_4 and NaOH solution, and the conductivity of simulated wastewater is adjusted by anhydrous sodium sulfate. The card slots inside the reactor are, respectively, inserted into the anode and cathode, wherein the anode is made of titanium-based plate and the cathode is made of graphite plate. The two electrodes are placed in parallel, the distance between the plates is 5 cm, the size of the electrode plate is 70 mm × 100 mm, and their effective area is 63 cm^2. A certain amount of Ti-Ag/γ-Al_2O_3 particle electrodes are added to the reaction tank before the test to form a three-dimensional electrodegradation system. 450 mL of chloramphenicol simulated wastewater is taken into the reactor, and the power supply of the electrolysis is turned on. The aeration device and power supply are opened with adjusting the aeration amount and current intensity. Water sampling is collected at every 30 min to analyze the concentration of chloramphenicol. The chloramphenicol is detected by ultraviolet spectrophotometry, UV–Vis spectra of chloramphenicol are shown in Fig. S1. In order to avoid the influence of particle electrode adsorption on electrocatalytic experiments, adsorption experiments of particle electrodes are carried out before electrocatalytic experiments. As shown in Fig. S2, γ-Al_2O_3 particle could not effectively adsorb chloramphenicol. It is also found that the removal rate by adsorption increases gradually and becomes stable after 120 min, indicating that the adsorption of chloramphenicol by γ-Al_2O_3 is saturated with only 4.4% removal rate by adsorption at 180 min.

3. Results and discussion

3.1. Preparation of Ti-Ag/γ-Al_2O_3 particle electrode

Ti and Ag are combined and loaded onto the surface of γ-Al_2O_3 particle. The chloramphenicol removal rate is selected as evaluation index to investigate the three-dimensional electrocatalytic degradation of Ti-Ag/γ-Al_2O_3 particle electrodes prepared under different Ti/Ag ratios, loading times and calcination temperatures in Figs. S3–S5. Experimental studies on chloramphenicol removal for optimization of preparation process of Ti-Ag/γ-Al_2O_3 particle electrodes show the optimum preparation process as follows: mass ratio of Ti/Ag = 50:5, loading times 2, and the calcination temperature 450°C.

3.2. Characterization of Ti-Ag/γ-Al_2O_3

3.2.1. SEM characterization

The surface of blank γ-Al_2O_3 is relatively smooth and has obvious spatial pore structure. The surface of Ti-Ag/γ-Al_2O_3 prepared at calcination temperature 250°C has no obvious crystal or particle formation, and the surface of Ti-Ag/γ-Al_2O_3 prepared by calcination at 350°C has a little crystal formation, indicating that the crystal growth is slow under low temperature conditions with small active component [18]. The obvious crystals and particles can be observed on the surface of Ti-Ag/γ-Al_2O_3 prepared by calcination at 450°C, wherein the crystals are TiO_2 and Ag_2O, and the particles are Ag elemental particles. And the crystals and particles are distributed on the surface and the pores of Ti-Ag/γ-Al_2O_3 with good dispersibility [21]. When the calcination temperature is 550°C, significant increase of the crystal and particle size on the surface of Ti-Ag/γ-Al_2O_3 can be obviously observed with coating phenomenon, but it still has a certain spatial structure [22]. When the temperature continues to increase to 650°C and 750°C, the surface of Ti-Ag/γ-Al_2O_3 is heavily coated with even obvious plate-forming phenomenon and fuzzy spatial structure. The Ti-Ag/γ-Al_2O_3 calcined at 750°C shows similar microscopic morphology even to the blank γ-Al_2O_3.

3.2.2. XRF and EDS characterization

It can be seen from Table 1 that the load-active metal content is greatly improved, wherein the atomic weight of Ti and Ag element is as high as 1.67% and 0.33%, respectively, indicating the formation of catalytically active Ag_2O and TiO_2 crystal. It can be observed from Fig. S6 that the characteristic peak of Ag element appears at 14°, and the characteristic peak of Ti element appears at 77° and 86°, indicating that the active components have been successfully loaded on the surface of γ-Al_2O_3 [23]. It can be seen from Table 2

Table 1
Main element composition of γ-Al_2O_3 and Ti-Ag/γ-Al_2O_3 particle electrodes by EDX

Sample	γ-Al_2O_3		Ti-Ag/γ-Al_2O_3	
Element	Mass percentage (%)	Atomic percentage (%)	Mass percentage (%)	Atomic percentage (%)
O K	46.23	58.54	38.75	56.48
Al K	52.50	40.73	47.45	39.24
Si K	0.40	0.31	–	–
Ti K	–	–	4.93	1.67
Ag K	–	–	1.78	0.33

Table 2
Main oxide composition of γ-Al_2O_3 and Ti-Ag/γ-Al_2O_3 particle electrodes by XRF

Name	Al_2O_3	SiO_2	CaO	TiO_2	Ag_2O
γ-Al_2O_3 (%)	99.881	0.042	0.031	0	0
Ti-Ag/γ-Al_2O_3 (%)	96.792	0.037	0.027	2.16	0.13

that the weight of TiO_2 and Ag_2O after loading are 2.16% and 0.13%, respectively.

3.2.3. XRD characterization

It can be seen from Fig. 2, When the calcination temperature is 250°C, the XRD pattern of Ti-Ag/γ-Al_2O_3 only shows low-intensity Ag_2O and silver elemental diffraction peaks

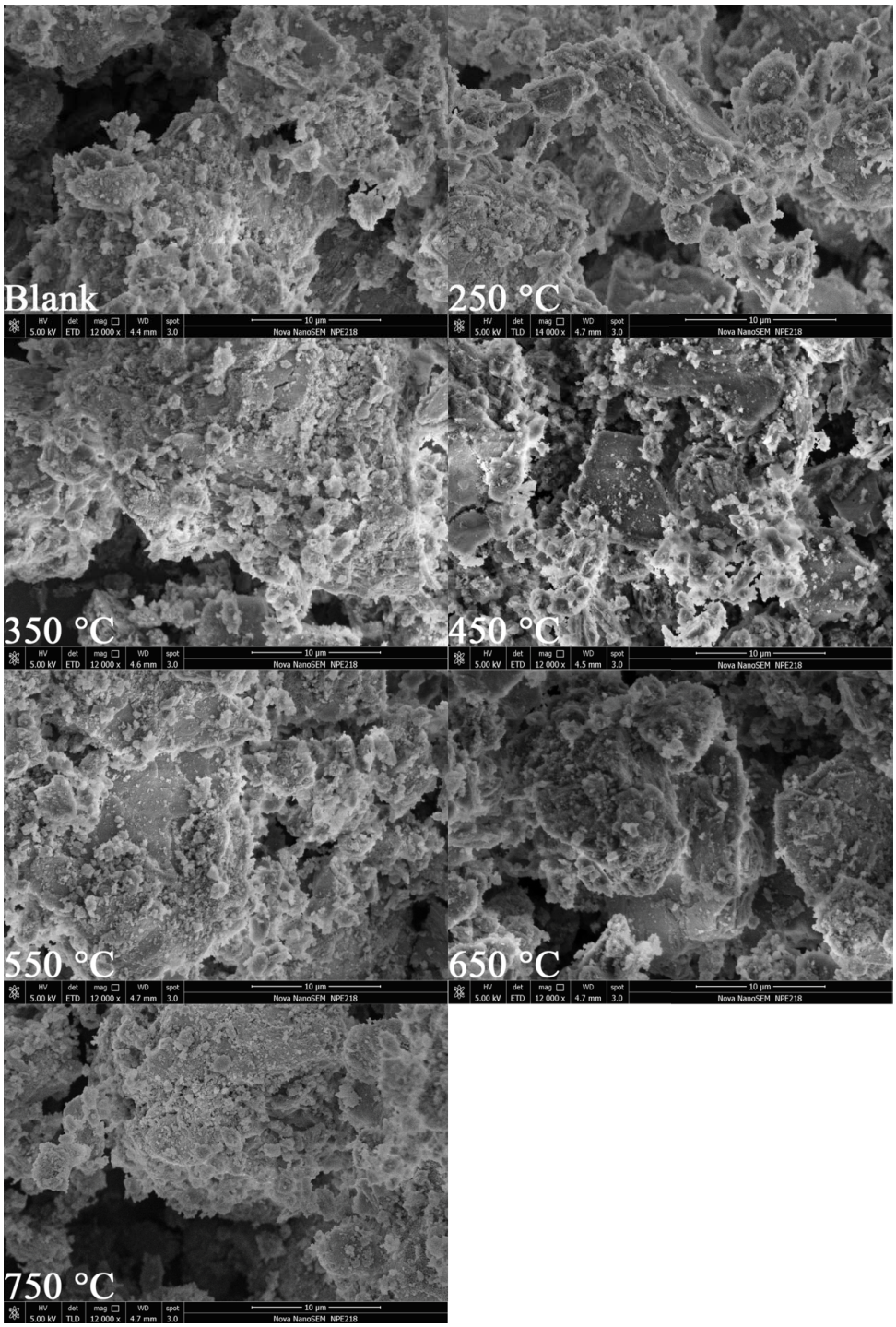

Fig. 1. Surface morphology of Ti-Ag/γ-Al_2O_3 particle electrodes at different temperatures.

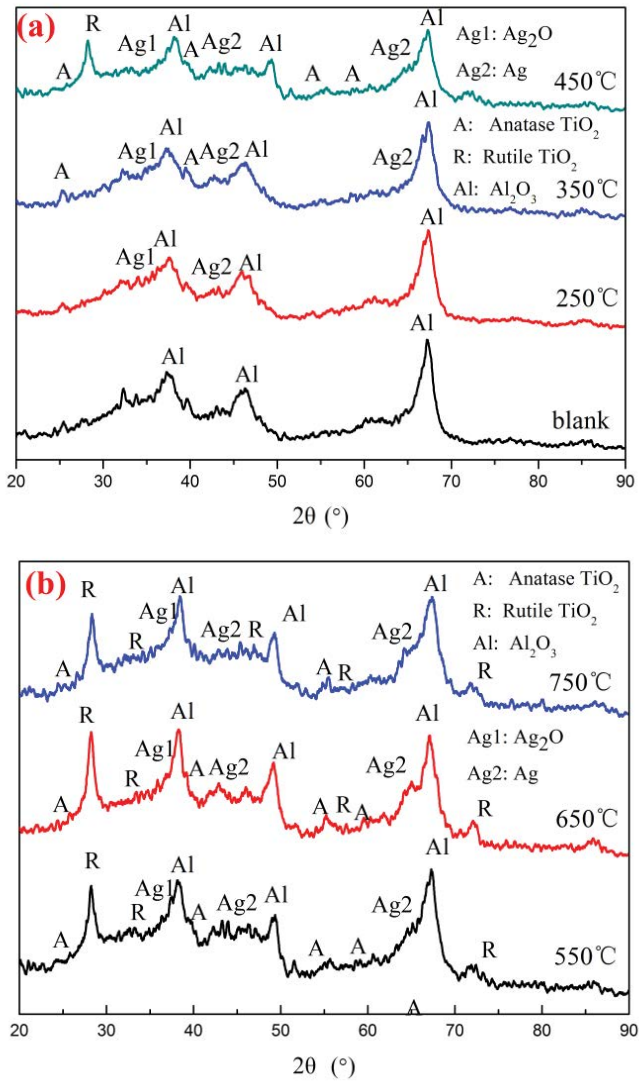

Fig. 2. XRD spectra of Ti-Ag/γ-Al_2O_3 particle electrode at different temperatures.

at 2θ = 38.6° and 44.0°, respectively, and the other parts are basically consistent with the XRD pattern of blank γ-Al_2O_3. When the temperature is 350°C, the intensity of the diffraction peak of silver element is enhanced. The characteristic diffraction peak of Ag_2O crystal appears at 2θ = 38.6°, and the characteristic diffraction peak of silver element appears at 2θ = 44.0° and 64.1° [24]. In addition, the characteristic diffraction peak of low-intensity anatase TiO_2 appears at 2θ = 25.3° and 37.8°, which indicates that the proper increase of the calcination temperature is beneficial to the formation of the active component [25]. When the calcination temperature is 450°C, both the quantity and the strength of various characteristic peaks have been greatly improved, and the intensity peaks of Ag_2O crystals and silver are enhanced at 2θ = 38.6° and 2θ = 44.0°, 64.1°, respectively [26]. A high-intensity diffraction peaks of anatase TiO_2 appear at 2θ = 25.3° and 37.8°, and a diffraction peak of rutile TiO_2 appears at 2θ = 27.5°. When the calcination temperature is 550°C, the number of diffraction peaks of anatase TiO_2, Ag_2O crystals, and silver element do not increase, but the width of each characteristic peaks became significantly small, indicating that the size of the active component supported on the surface of the substrate became large and catalytic activity decreases [27]. In addition, the number and the intensity of diffraction peaks of rutile TiO_2 corresponding to 2θ = 27.5° and 36.1° with poor catalytic activity increases [28]. When the calcination temperature is increased to 650°C and 750°C, the characteristic diffraction peak widths of anatase TiO_2, Ag_2O crystals, and silver continue to narrow, and the number and intensity of characteristic peaks of anatase TiO_2 decrease [29]. At the same time, the characteristic peaks of rutile TiO_2 appear at 2θ = 27.5°, 36.1°, 56.7°, and 73.5° in large quantities, and their intensities become large, which indicates that the size of the active component supported on the surface gradually increases as the calcination temperature increases with decreasing catalytic activity [30].

Through the above analysis, it can be found that the crystals appear not to be obvious under low temperature conditions. As the calcination temperature increases, the amount and size of the active components supported on the surface gradually increases and the existence form of TiO_2 also shift, which is consistent with the results of the aforementioned chloramphenicol degradation test by Ti-Ag/γ-Al_2O_3 particle electrode at different calcination temperatures.

3.3. Single-factor studies of operation condition of three-dimensional electrocatalytic system

3.3.1. Effect of conductivity

It can be seen from Fig. 3 that the conductivity of the solution has a great influence on the degradation of chloramphenicol. With the increase of the conductivity of the solution, the removal rate of chloramphenicol first increases and then decreases, and the optimal removal rate is 67.4% at 6,000 μs cm^{-1}. The removal rate decreased with continuously increasing conductivity. This may be due to two reasons: (1) when the conductivity is high, the large concentration of electrolyte is easily adsorbed by Ti-Ag/γ-Al_2O_3 particle

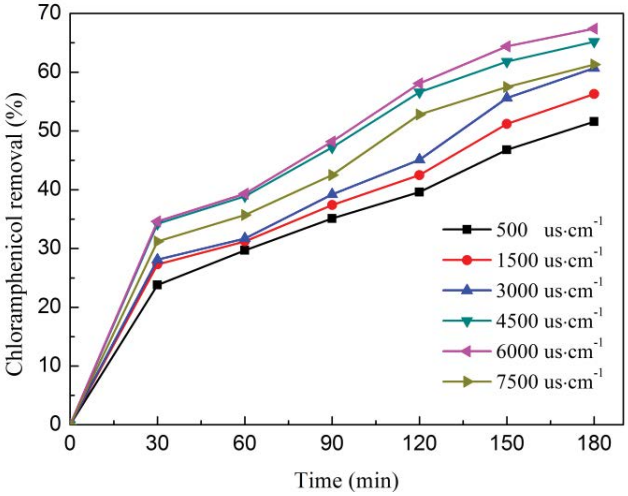

Fig. 3. Effect of electrical conductivity on chloramphenicol removal efficiency.

electrode, thereby causing the encapsulation of the active component of Ti-Ag/γ-Al_2O_3 particle electrode, reducing the probability contact of the active center and chloramphenicol [31]. (2) In the three-dimensional electrolysis system, the bypass current increases with the increase of conductivity, so that the reaction current involved in degradation is continuously reduced, thereby reducing the electrocatalytic efficiency [32].

3.3.2. Effect of pH

As shown in Fig. 4, the pH of the solution has a great influence on the degradation of chloramphenicol. As a whole, the degradation of chloramphenicol under acidic conditions is significantly better than that under alkaline conditions. The optimal removal rate of chloramphenicol reaches 78.6% at pH 4.0. This is mainly due to that it is beneficial to the formation of •OH during the electrolysis process under acidic conditions. However, when the acidity continues to increase, the removal rate of chloramphenicol is not obvious. When, the removal rate of chloramphenicol reaches 79.2% at pH 2.0, because a large amount of H^+ produces side reactions at the cathode, so that the conductivity of the solution is continuously decreased, thereby reducing the degradation efficiency of chloramphenicol.

The high removal rate of chloramphenicol is obtained in strong acidity of the solution. But when the pH is lower than 4.0, the degradation rate of chloramphenicol is not obvious, and the long-term reaction in the peracid environment will greatly reduce service life of the equipment [33]. In addition, the maintenance of the acid environment also requires a large amount of pharmaceutical costs, so pH 4.0 is selected as the initial pH of the solution for this experiment.

3.3.3. Effect of current intensity

It can be seen from Fig. 5 that the removal rate of chloramphenicol increases first and then decreases with the increase of current intensity. When the removal rate of chloramphenicol reaches the maximum value of 88.4% at I = 0.3 A, and compared with I = 0.2 A, the removal rate increases by only 2.1%. When the current intensity continues to increase, it is more obvious that a large amount of bubbles escape in the water. This is because the excessive current intensity makes the electrolysis side reaction increase sharply. The effective current utilization rate and utilization efficiency of intermediate products continuously decrease, thereby reducing the degradation efficiency of chloramphenicol. The current intensity is one of the important factors in the three-dimensional electrocatalytic reaction [34]. It directly affects the progress of the electrocatalytic reaction. The decrease of the current intensity leads to the oxidation of the main plate of the electrocatalytic process and the decrease of the yield of the intermediate product, which in turn affects the catalytic efficiency [35]. When the strength is too high, on the one hand, the electrolysis side reaction is greatly enhanced, affecting the utilization efficiency of the intermediate product, thereby reducing the electrocatalytic efficiency [36]. And on the other hand, the ineffective current such as the bypass current and the short-circuit current increase, leading to the great increase of electrolysis energy consumption [37].

3.3.4. Effect of aeration intensity

As shown in Fig. 6 that the removal rate of chloramphenicol increases with the increase of air flow rate. Under the condition of no aeration, the removal rate of chloramphenicol is only 56.2%, and when the air flow rate is increased to 1.0 L/min, the removal rate of chloramphenicol increases to 84.2%, indicating that the proper increase of oxygen concentration is beneficial to improve the electrocatalytic efficiency and the removal rate of chloramphenicol. However, when the air flow rate continues to increase, the removal rate of chloramphenicol is no longer obvious. When the air flow rate is 4.0 L/min, the removal rate of chloramphenicol increases to 87.9%, which is only 3.7% more than that at 1.0 L/min, indicating the utilization rate of oxygen in the whole reaction system has become saturated at air flow rate 1.0 L/min. It is not meaningful to continue to

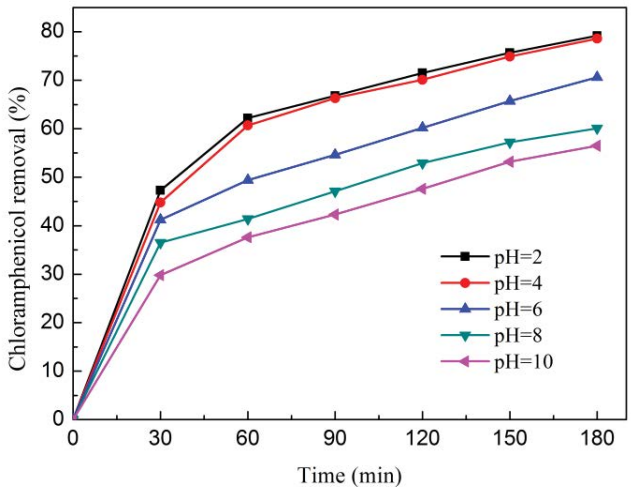

Fig. 4. Effect of pH value on chloramphenicol removal efficiency.

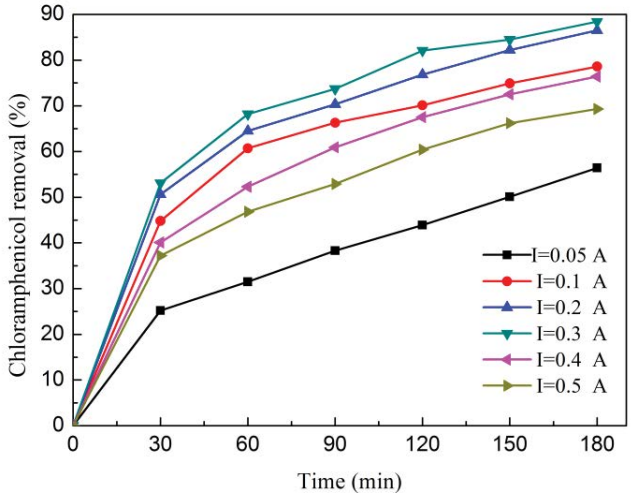

Fig. 5. Effect of current intensity value on chloramphenicol removal efficiency.

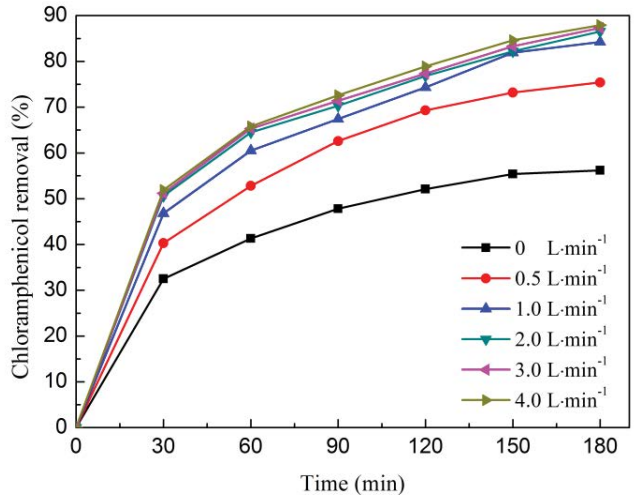

Fig. 6. Effect of air flow value on chloramphenicol removal efficiency.

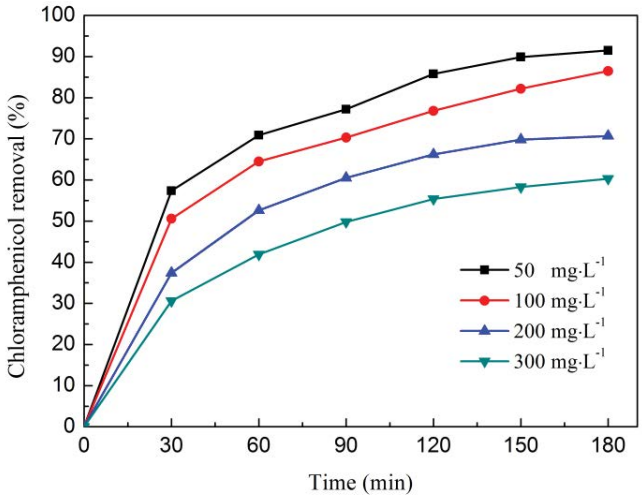

Fig. 7. Effect of different initial concentration on three-dimensional electrocatalytic removal of chloramphenicol.

increase the air flow rate, so the air flow rate is determined to be 1.0 L/min for subsequent experiments.

The addition of aeration in the three-dimensional electrocatalytic system has two main functions: (1) aeration can promote the flow of water and achieve a homogeneous function [38]; (2) in the electrocatalytic process, high oxygen concentration in water can inhibit the oxygen evolution reaction of the anode, and oxygen can also generate H_2O_2 at the cathode, thereby improving •OH yield and the degradation efficiency of chloramphenicol [34].

3.3.5. Effect of initial concentration of chloramphenicol

It can be seen from Fig. 7 that the degradation rate of chloramphenicol decreases with the increase of initial concentration. When the initial concentration of chloramphenicol is 50 mg/L, the removal rate of chloramphenicol is 91.5%. However, when the initial concentration increases to 300 mg/L, the removal rate of chloramphenicol reduces to 60.3%, indicating that the initial concentration of chloramphenicol had a great effect on the degradation rate of chloramphenicol. This is because the excessive concentration of chloramphenicol causes excessive degradation of chloramphenicol and intermediates on the surface of Ti-Ag/γ-Al_2O_3 particle electrode, so that the active center cannot sufficiently perform electrocatalytic oxidation reaction, reducing the generated active radicals and the degradation rate of chloramphenicol [39]. If the concentration of organic pollutants in the solution is too large, it will cause excessive adsorption of pollutants on the surface of Ti-Ag/γ-Al_2O_3 particle electrode, decreasing catalytic activity of active center [40].

3.3.6. Discussion on direct oxidation and indirect oxidation

In order to verify the intermediate product •OH produced in the entire electrocatalytic reaction, the hydroxyl radical eliminating agent *t*-butanol is used for verification experiments. It can be seen from Fig. 8 that the addition of *t*-butanol has a great influence on the degradation rate of chloramphenicol. When 50 mg/L of *t*-butanol is added, the

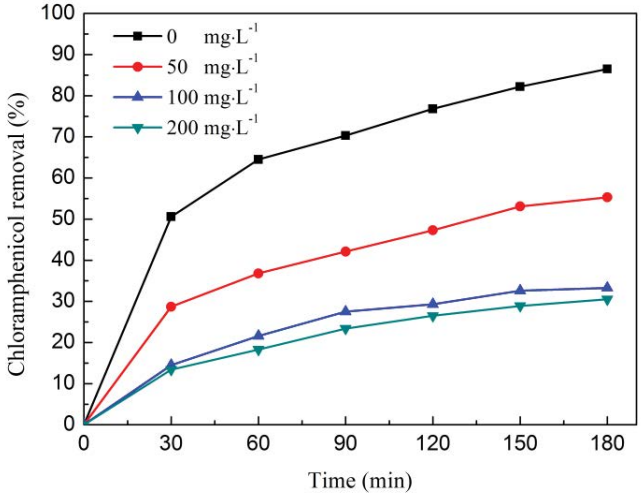

Fig. 8. Degradation of chloramphenicol in the presence of tert-butanol.

removal rate of chloramphenicol suddenly drops to 55.3%. And when the amount of *t*-butanol reaches 100 mg/L, the removal rate of chloramphenicol is only 34.3%. However, the dosage of *t*-butanol continues to increase, and the removal rate of chloramphenicol does not change much. This is because the generated •OH has been basically eliminated by *t*-butanol [41]. Through the above experiments, it can be obtained that the three-dimensional electrocatalytic system degrading chloramphenicol is a multi-channel synergistic reaction process, in which •OH plays a major role, and anodization and cathodic reduction are auxiliary functions [42].

In addition, the degradation rate of chloramphenicol was faster in the first 90 min, and then gradually became stable under the above optimal operating conditions, and the optimal removal rate of chloramphenicol reaches 84.2% at 180 min in Fig. S7. The results show that the

three-dimensional electrocatalytic system has good removal capacity of chloramphenicol. As shown in Fig. S8, the reaction time has a good linear relationship with Ln(C/C_0) with fitting degree R^2 = 0.995. Therefore, it can be considered that this catalytic degradation reaction conforms to the first-order kinetic model.

The operation condition was set with initial concentration of chloramphenicol 100 mg/L, conductivity 6,000 μs cm^{-1}, initial pH 4.0, current intensity I = 0.2 A, and flow rate 1.0 L/min. After each electrocatalytic oxidation for 180 min, the catalyst used in the test was repeatedly washed and dried in an oven for the next electrocatalytic oxidation experiment. The Ti-Ag/γ-Al_2O_3 particles were subjected to five repeated tests to obtain a chloramphenicol degradation rate per time. The chloramphenicol removal rate after the five replicates is shown in Fig. S9. It can be seen from Fig. S9 that the electrocatalytic oxidation efficiency of Ti-Ag/γ-Al_2O_3 particle has a certain degree of decrease in catalytic performance with the increase in utilization times. But the decrease in catalytic performance is not large and tends to be gentle. At the fifth utilization, the removal rate of chloramphenicol was still 54.3%. The electrocatalytic oxidation efficiency of Ti-Ag/γ-Al_2O_3 particles after five utilization times decreases by about 11.0%.

It can be seen from Table S2 that the quantitative analysis of Ti-Ag/γ-Al_2O_3 particles after five utilization times, the atomic weight of Ti is as high as 1.39%, and the atomic weight of Ag is 0.27%, indicating that the active component of Ti-Ag/γ-Al_2O_3 particles loses less during three-dimensional electrocatalytic degradation. In addition, we also tested the concentration of Ti and Ag in the wastewater during the electrocatalytic oxidation experiment, but we did not detect Ti and Ag in the wastewater. The above results indicate the loss of Ti and Ag during the electrocatalytic oxidation process, but it may be precipitated as the solid form in the wastewater. This may be caused by friction between the Ti-Ag/γ-Al_2O_3 particle electrodes due to aeration caused by aeration, which causes the supported Ti and Ag active component oxides to detach from the surface of the three-dimensional particle electrode.

4. Conclusions

In this paper, Ti-Ag/γ-Al_2O_3 particle electrodes are prepared for three-dimensional electrocatalytic degradation of chloramphenicol. The optimal conditions for preparing Ti-Ag/γ-Al_2O_3 particle electrodes are that: mass ratio of Ti/Ag = 50:1, the loading times two, and the calcination temperature 450°C. It is found by characterization that the crystal form of Ti-Ag/γ-Al_2O_3 particle electrodes changes with temperature and has a certain content of electrocatalytic active components on surface of Ti-Ag/γ-Al_2O_3 particle electrodes. The optimum operating conditions for the three-dimensional electrocatalytic degradation of chloramphenicol using the prepared Ti-Ag/γ-Al_2O_3 particle electrodes are as following: initial concentration of chloramphenicol 100 mg/L, conductivity 6,000 μs cm^{-1}, initial pH = 4.0, current intensity I = 0.2 A, air flow rate 1.0 L/min; the optimal removal rate of chloramphenicol at this time is 84.2%, and the degradation process of chloramphenicol in the electrocatalytic system is approximately in accordance with the first-order kinetic equation. In the degradation system, hydroxyl radicals produced during the electrocatalytic process play a major role for degrading chloramphenicol, and the entire degradation process is carried out under the combined action of the indirect oxidation of •OH and the direct oxidation of the electrocatalytic anode. This research has important practical significance for the further popularization and application of three-dimensional electrocatalytic technology.

Acknowledgements

This research was supported by National Natural Science Foundation of China (No. 51508268), National Key Research and Development Program of China (2017YFB0602500), and 2018 Six Talent Peaks Project of Jiangsu Province (JNHB-038).

References

[1] M. Zhang, Y. Liu, J. Zhao, W. Liu, L. He, J. Zhang, J. Chen, L. He, Q. Zhang, G. Ying, Occurrence, fate and mass loadings of antibiotics in two swine wastewater treatment systems, Sci. Total Environ., 639 (2018) 1421–1431.
[2] W. Zhang, D. Xie, X. Li, W. Ye, X. Jiang, Y. Wang, W. Liang, Electrocatalytic removal of humic acid using cobalt-modified particle electrodes, Appl. Catal. A-Gen., 559 (2018) 75–84.
[3] P.M. Shafi, N. Joseph, A. Thirumurugan, A.C. Bose, Enhanced electrochemical performances of agglomeration-free $LaMnO_3$ perovskite nanoparticles and achieving high energy and power densities with symmetric supercapacitor design, Chem. Eng. J., 338 (2018) 147–156.
[4] B. Xu, Y. Zhai, W. Chen, B. Wang, T. Wang, C. Zhang, C. Li, G. Zeng, Perchlorate catalysis reduction by benzalkonium chloride immobilized biomass carbon supported Re-Pd bimetallic cluster particle electrode, Chem. Eng. J., 348 (2018) 765–774.
[5] J.V. Kumar, R. Karthik, S. Chen, K. Chen, S. Sakthinathan, V. Muthuraj, T. Chiu, Design of novel 3D flower-like neodymium molybdate: an efficient and challenging catalyst for sensing and destroying pulmonary toxicity antibiotic drug, Chem. Eng. J., 346 (2018) 11–23.
[6] W. Sun, B. Ma, Y. Sun, H. Zheng, G. Ma, Electrochemical degradation of tetracycline by gamma-Al_2O_3-Bi-(Sn/Sb) three-dimensional particle electrode, Desal. Wat. Treat., 98 (2017) 152–160.
[7] K.P. de Amorim, L.L. Romualdo, L.S. Andrade, Electrochemical degradation of sulfamethoxazole and trimethoprim at boron-doped diamond electrode: performance, kinetics and reaction pathway, Sep. Purif. Technol., 120 (2013) 319–327.
[8] A.A. Ensafi, A.R. Allafchian, B. Rezaei, Multiwall carbon nanotubes decorated with $FeCr_2O_4$, a new selective electrochemical sensor for amoxicillin determination, J. Nanopart. Res., 14 (2012) 1244.
[9] F. Yuan, C. Hu, X. Hu, D. Wei, Y. Chen, J. Qu, Photodegradation and toxicity changes of antibiotics in UV and UV/H_2O_2 process, J. Hazard. Mater., 185 (2011) 1256–1263.
[10] A.S. Kumar, S. Sornambikai, S. Venkatesan, J. Chang, J. Zen, Tetracycline immobilization as hydroquinone derivative at dissolved oxygen reduction potential on multiwalled carbon nanotube, J. Electrochem. Soc., 159 (2012) G137–G145.
[11] C. Liu, D. Fu, H. Li, Behaviour of multi-component mixtures of tetracyclines when degraded by photoelectrocatalytic and electrocatalytic technologies, Environ. Technol., 33 (2012) 791–799.
[12] C. Zhao, B. Si, Z.A. Mirza, Y. Liu, X. He, J. Li, Z. Wang, H. Zheng, Activated carbon fiber (ACF) enhances the UV/EF system to remove nitrobenzene in water, Sep. Purif. Technol., 187 (2017) 397–406.
[13] Z. Liu, C. Zhao, P. Wang, H. Zheng, Y. Sun, D.D. Dionysiou, Removal of carbamazepine in water by electro-activated carbon fiber-peroxydisulfate: comparison, optimization, recycle, and mechanism study, Chem. Eng. J., 343 (2018) 28–36.

[14] C.A. Little, R. Xie, C. Batchelor-McAuley, E. Kaetelhoen, X. Li, N.P. Young, R.G. Compton, A quantitative methodology for the study of particle-electrode impacts, Phys. Chem. Chem. Phys., 20 (2018) 13537–13546.
[15] J. Losada, M.P. Garcia Armada, E. Garcia, C.M. Casado, B. Alonso, Electrochemical preparation of gold nanoparticles on ferrocenyl-dendrimer film modified electrodes and their application for the electrocatalytic oxidation and amperometric detection of nitrite, J. Electroanal. Chem., 788 (2017) 14–22.
[16] Y. Yang, H. Zeng, W.S. Huo, Y.H. Zhang, Direct electrochemistry and catalytic function on oxygen reduction reaction of electrodes based on two kinds of magnetic nano-particles with immobilized laccase molecules, J. Inorg. Organomet. Polym. Mater., 27 (2017) 201–214.
[17] Y. Sun, P. Li, H. Zheng, C. Zhao, X. Xiao, Y. Xu, W. Sun, H. Wu, M. Ren, Electrochemical treatment of chloramphenicol using Ti-Sn/gamma-Al_2O_3 particle electrodes with a three-dimensional reactor, Chem. Eng. J., 308 (2017) 1233–1242.
[18] M. Tian, S.S. Thind, J.S. Dondapati, X.Y. Li, A.C. Chen, Electrochemical oxidation of 4-chlorophenol for wastewater treatment using highly active UV treated TiO_2 nanotubes, Chemosphere, 209 (2018) 182–190.
[19] E.Y. Jo, T.K. Lee, Y. Kim, C.G. Park, Effect of anions on the removal of bisphenol A in wastewater by electro-oxidation process, Desal. Wat. Treat., 57 (2016) 29500–29508.
[20] N. Flores, I. Sires, R.M. Rodriguez, F. Centellas, P.L. Cabot, J.A. Garrido, E. Brillas, Removal of 4-hydroxyphenylacetic acid from aqueous medium by electrochemical oxidation with a BDD anode: mineralization, kinetics and oxidation products, J. Electroanal. Chem., 793 (2017) 58–65.
[21] S. Wu, K.S. Hui, K.N. Hui, J.M. Yun, K.H. Kim, Silver particle-loaded nickel oxide nanosheet arrays on nickel foam as advanced binder-free electrodes for aqueous asymmetric supercapacitors, RSC Adv., 7 (2017) 41771–41778.
[22] B. Hou, R. Deng, B. Ren, Z. Li, Facile preparation of a novel catalytic particle electrode from sewage sludge and its electrocatalytic performance in three-dimensional heterogeneous electro-Fenton, Water Sci. Technol., 76 (2017) 2350–2356.
[23] Y.Y. Ahn, S.Y. Yang, C. Choi, W. Choi, S. Kim, H. Park, Electrocatalytic activities of Sb-SnO_2 and Bi-TiO_2 anodes for water treatment: effects of electrocatalyst composition and electrolyte, Catal. Today, 282 (2017) 57–64.
[24] B. Hou, H. Han, S. Jia, H. Zhuang, P. Xu, K. Li, Three-dimensional heterogeneous electro-Fenton oxidation of biologically pre-treated coal gasification wastewater using sludge derived carbon as catalytic particle electrodes and catalyst, J. Taiwan Inst. Chem. E, 60 (2016) 352–360.
[25] Y. Feng, X. Wang, J. Qi, Y. Feng, Z. Wang, B. Wang, X. Li, Removal of ibuprofen from municipal sewage by three-dimensional particle electrode combined with a biological aerated filter (TDE-BAF), Desal. Wat. Treat., 57 (2016) 20470–20475.
[26] M. Que, W. Que, X. Yin, J. Shao, Enhanced sunlight harvesting of dye-sensitized solar cells through the insertion of a (Sr, Ba, Eu)$_2$ SiO_4-TiO_2 composite layer, Mater. Res. Bull., 83 (2016) 19–23.
[27] M. Romero-Arcos, M. Garnica-Romo, H. Martínez-Flores, Electrochemical study and characterization of an amperometric biosensor based on the immobilization of laccase in a nanostructure of TiO_2 synthesized by the sol-gel method, Materials, 9 (2016) 543.
[28] Y. Feng, X. Wang, J. Qi, Z. Wang, X. Li, Production of red mud particle electrodes (RMPEs) and its performance investigation in a biological aerated filter coupled with a three-dimensional particle electrode reactor (BAF-TDE), Ind. Eng. Chem. Res., 54 (2015) 6641–6648.
[29] M.J. Ndolomingo, R. Meijboom, Kinetics of the catalytic oxidation of morin on γ-Al_2O_3 supported gold nanoparticles and determination of gold nanoparticles surface area and sizes by quantitative ligand adsorption, Appl. Catal. B: Environ., 199 (2016) 142–154.
[30] D. Li, J. Tang, X. Zhou, J. Li, X. Sun, J. Shen, L. Wang, W. Han, Electrochemical degradation of pyridine by Ti/SnO_2–Sb tubular porous electrode, Chemosphere, 149 (2016) 49–56.
[31] G. Conte, P. Allegrini, M. Pacilli, S. Salvatori, T. Kononenko, A. Bolshakov, V. Ralchenko, V. Konov, Three-dimensional graphite electrodes in CVD single crystal diamond detectors: charge collection dependence on impinging beta-particles geometry, Nucl. Instrum. Meth. A, 799 (2015) 10–16.
[32] M. Li, F. Zhao, M. Sillanpaa, Y. Meng, D. Yin, Electrochemical degradation of 2-diethylamino-6-methyl-4-hydroxypyrimidine using three-dimensional electrodes reactor with ceramic particle electrodes, Sep. Purif. Technol., 156 (2015) 588–595.
[33] Y. Kusumawati, S. Koussi-Daoud, T. Pauporté, TiO_2/graphene nanocomposite layers for improving the performances of dye-sensitized solar cells using a cobalt redox shuttle, J. Photochem. Photobiol. A: Chem., 329 (2016) 54–60.
[34] K. Jung, M. Hwang, D. Park, K. Ahn, Performance evaluation and optimization of a fluidized three-dimensional electrode reactor combining pre-exposed granular activated carbon as a moving particle electrode for greywater treatment, Sep. Purif. Technol., 156 (2015) 414–423.
[35] Z. Wang, J. Qi, Y. Feng, K. Li, X. Li, Preparation of catalytic particle electrodes from steel slag and its performance in a three-dimensional electrochemical oxidation system, J. Ind. Eng. Chem., 20 (2014) 3672–3677.
[36] M. Nie, Y. Yang, Z. Zhang, C. Yan, X. Wang, H. Li, W. Dong, Degradation of chloramphenicol by thermally activated persulfate in aqueous solution, Chem. Eng. J., 246 (2014) 373–382.
[37] R. Mao, X. Zhao, H. Lan, H. Liu, J. Qu, Graphene-modified Pd/C cathode and Pd/GAC particles for enhanced electrocatalytic removal of bromate in a continuous three-dimensional electrochemical reactor, Water Res., 77 (2015) 1–12.
[38] G.T. Correa, A.A. Tanaka, M. Isabel Pividori, M.V. Boldrin Zanoni, Use of a composite electrode modified with magnetic particles for electroanalysis of azo dye removed from dyed hair strands, J. Electroanal. Chem., 782 (2016) 26–31.
[39] B. Hou, B. Ren, R. Deng, G. Zhu, Z. Wang, Z. Li, Three-dimensional electro-Fenton oxidation of N-heterocyclic compounds with a novel catalytic particle electrode: high activity, wide pH range and catalytic mechanism, RSC Adv., 7 (2017) 15455–15462.
[40] F. Li, D. Xie, Y. Zhao, L. Liu, W. Liang, Effects of adsorption properties of particle electrodes on the degradation of acid red 14 using three-dimensional electrode system, Desal. Wat. Treat., 78 (2017) 263–272.
[41] M. Ahmadi, H. Ramezani Motlagh, N. Jaafarzadeh, A. Mostoufi, R. Saeedi, G. Barzegar, S. Jorfi, Enhanced photocatalytic degradation of tetracycline and real pharmaceutical wastewater using MWCNT/TiO_2 nano-composite, J. Environ. Manage., 186 (2017) 55–63.
[42] B. Shen, X. Wen, X. Huang, Enhanced removal performance of estriol by a three-dimensional electrode reactor, Chem. Eng. J., 327 (2017) 597–607.

Supplementary information:

Table S1
Characteristic parameters of γ-Al_2O_3

Parameters	Shape	Particle size (mm)	Specific surface area ($m^2\ g^{-1}$)	Specific pore volume ($cm^3\ g^{-1}$)	Hole diameter (nm)
γ-Al_2O_3	Sphere	4.0–6.0	>260.0	>0.40	>7.5

Table S2
EDS characterization of Ti-Ag/γ-Al_2O_3 before and after electrocatalytic oxidation experiment

Sample element	Original Ti-Ag/γ-Al_2O_3		Ti-Ag/γ-Al_2O_3 after five utilization times	
	Weight percentage	Atomic percentage	Weight percentage	Atomic percentage
O K	38.75	56.48	36.67	47.11
Al K	47.45	39.24	42.97	32.67
Si K	–	–	–	–
Ti K	4.93	1.67	4.11	1.39
Ag K	1.78	0.33	1.46	0.27

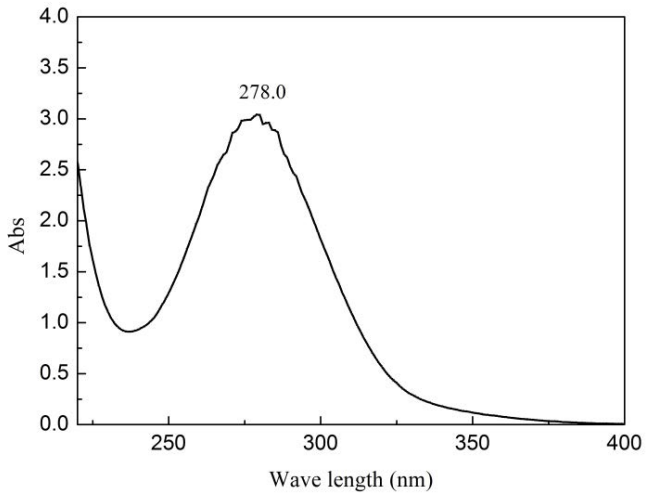

Fig. S1. UV–Vis spectra of chloramphenicol.

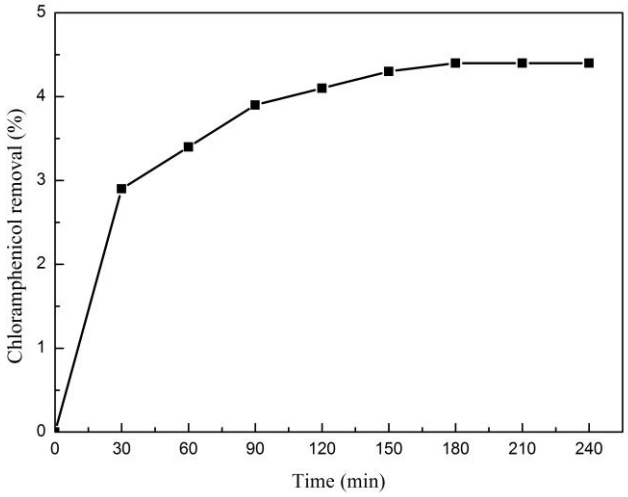

Fig. S2. Adsorption of chloramphenicol by γ-Al_2O_3.

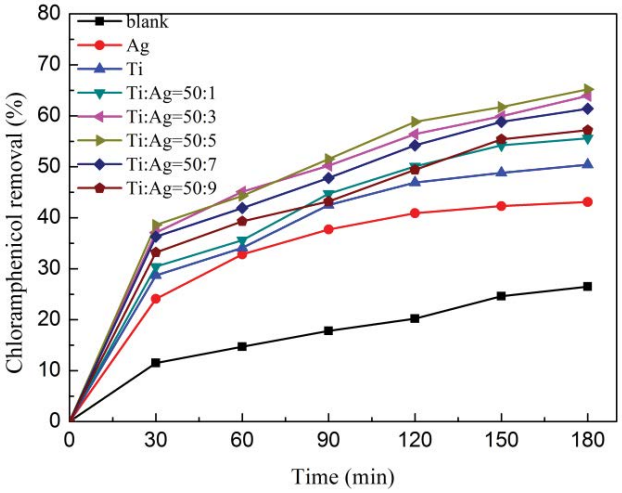

Fig. S3. Effect of mass ratio of Ti/Ag on chloramphenicol removal.

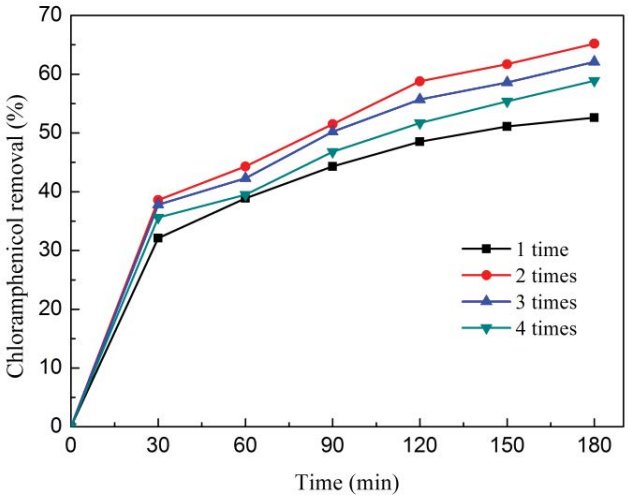

Fig. S4. Effect of load times on chloramphenicol removal.

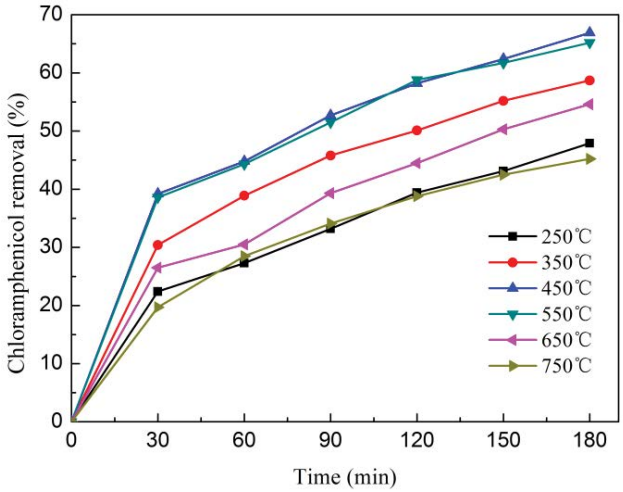

Fig. S5. Effect of calcination temperature on chloramphenicol removal.

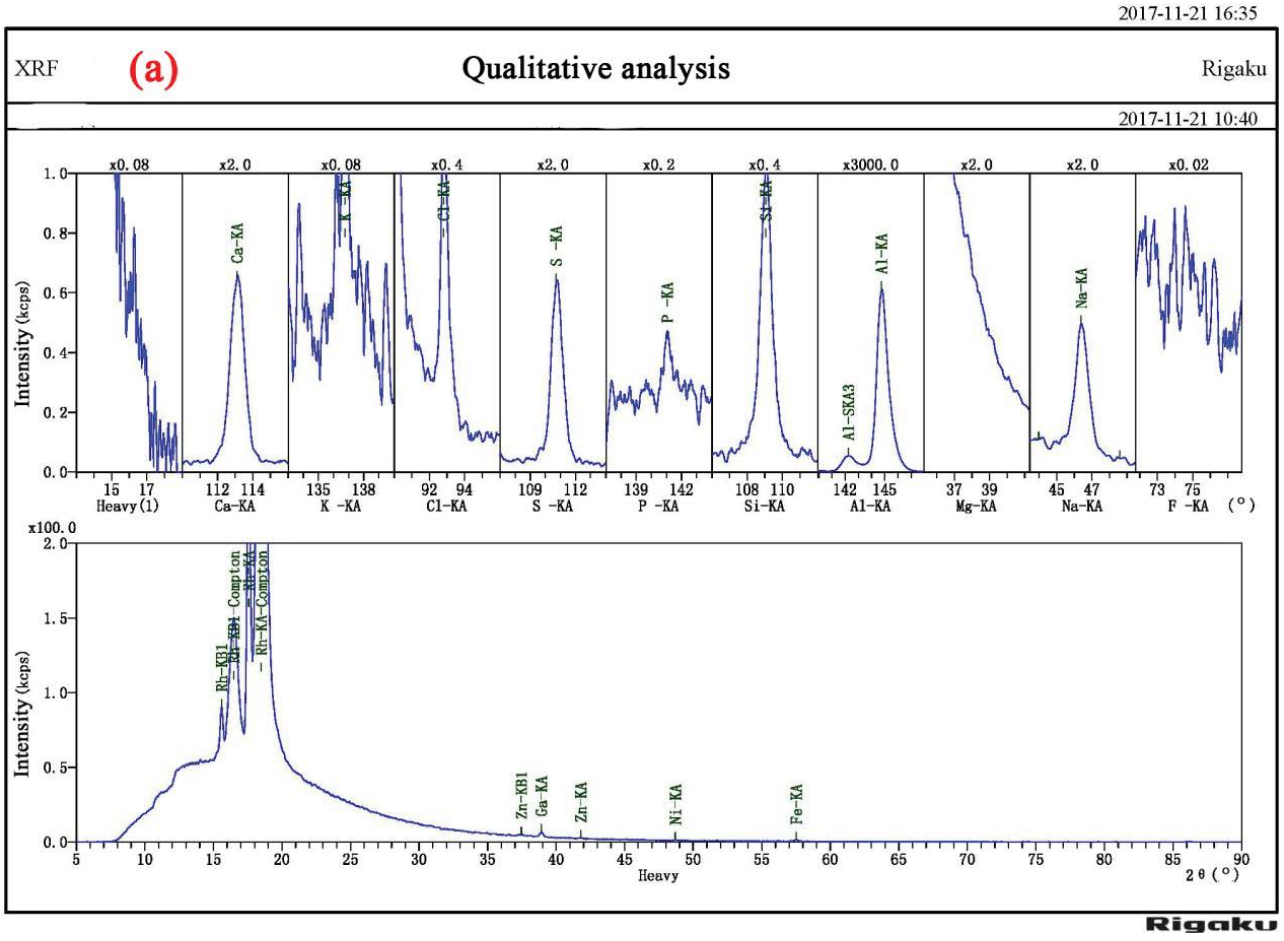

(*Continued*)

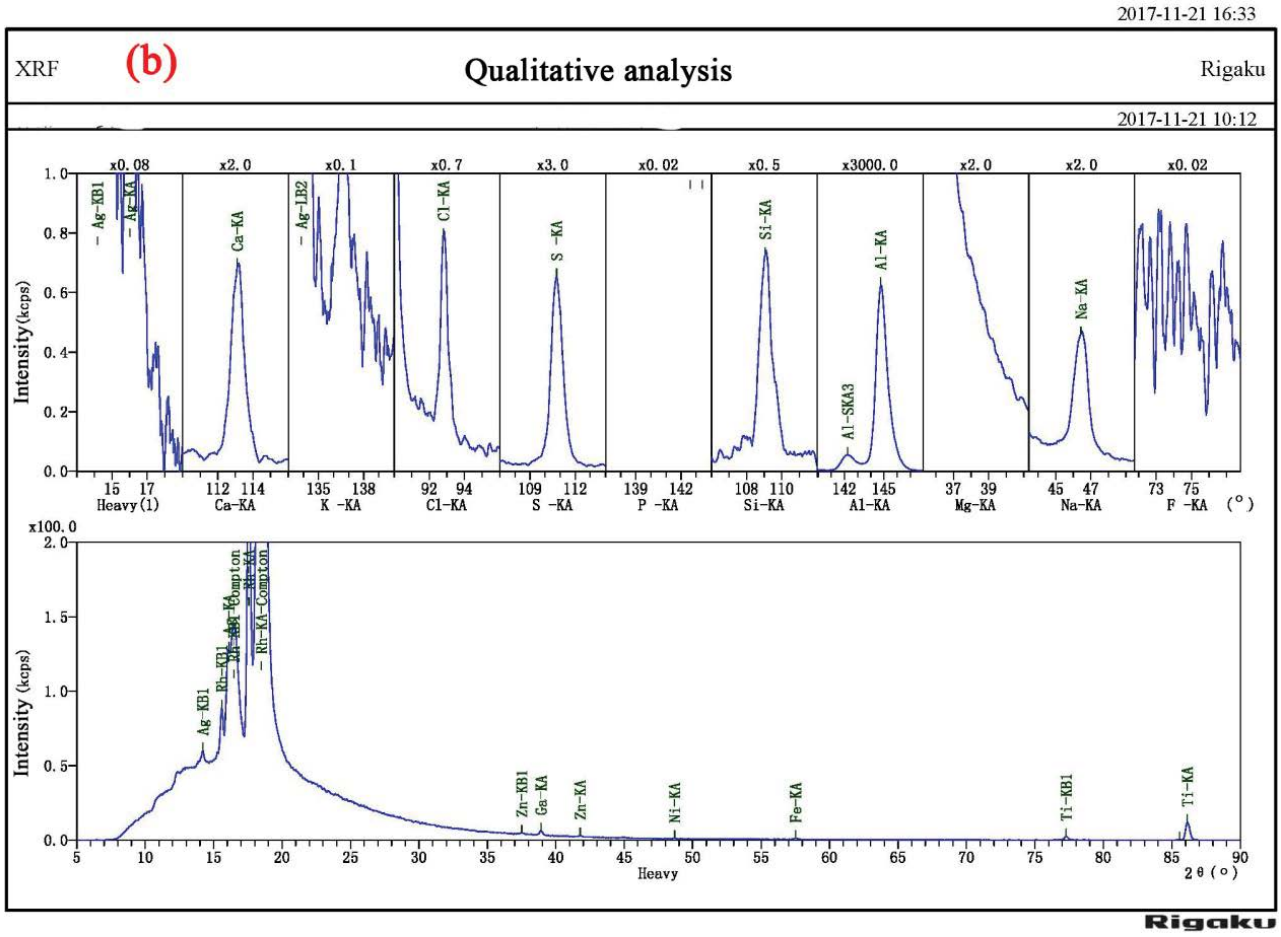

Fig. S6. XRF measurement of (a) γ-Al_2O_3 and (b) Ti-Ag/γ-Al_2O_3 particle electrodes.

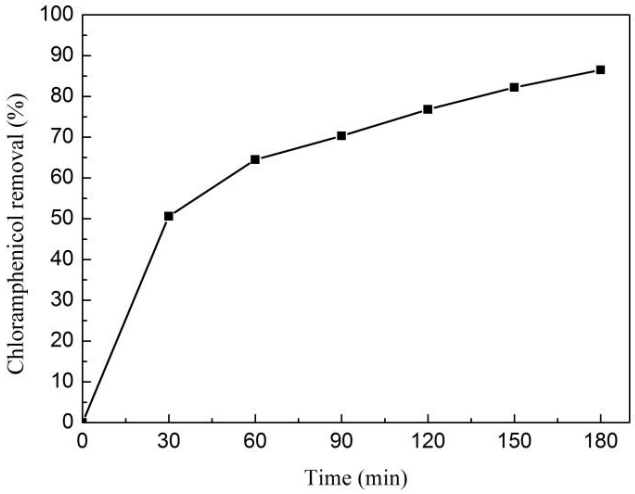

Fig. S7. Removal of chloramphenicol under optimal operating conditions.

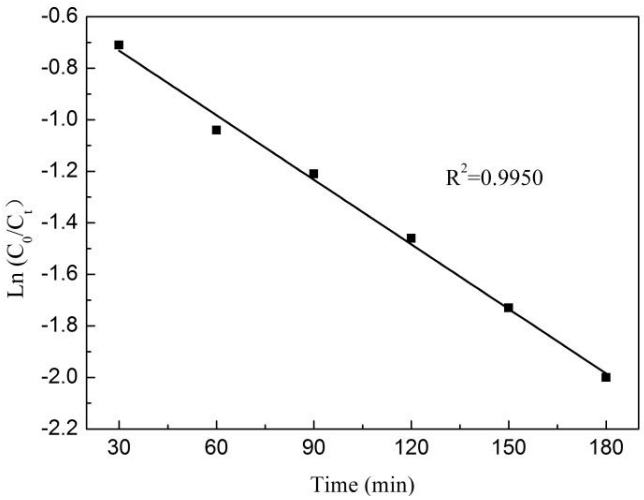

Fig. S8. Kinetic trend line of chloramphenicol under optimal operating conditions.

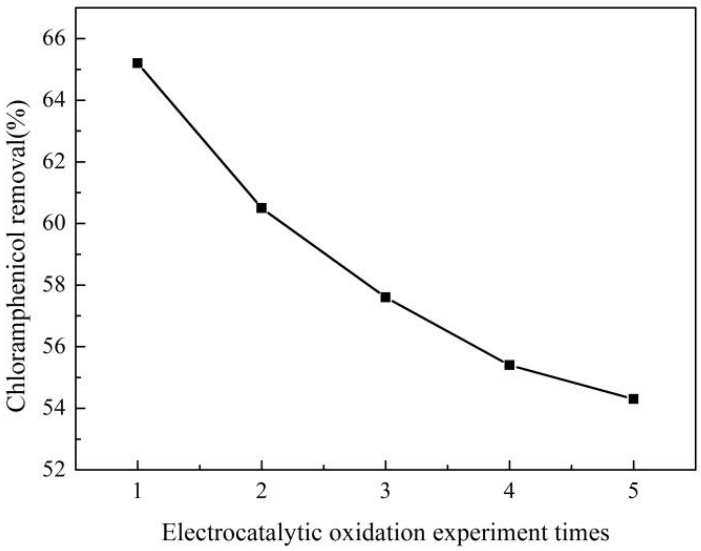

Fig. S9. Effect of electrocatalytic oxidation experiment times on the removal of chloramphenicol.